

2013

Holocarboxylasesynthetase interacts physically with euchromatic histone-lysine N-methyltransferase, linking histone biotinylation with methylation events

Yong Li

University of Nebraska-Lincoln

Yousef I. Hassan

University of Nebraska at Lincoln

Hideaki Moriyama

University of Nebraska-Lincoln, hmoriyama2@unl.edu

Janos Zempleni

University of Nebraska-Lincoln, jzempleni2@unl.edu

Follow this and additional works at: <http://digitalcommons.unl.edu/bioscifacpub>

Li, Yong; Hassan, Yousef I.; Moriyama, Hideaki; and Zempleni, Janos, "Holocarboxylasesynthetase interacts physically with euchromatic histone-lysine N-methyltransferase, linking histone biotinylation with methylation events" (2013). *Faculty Publications in the Biological Sciences*. 449.

<http://digitalcommons.unl.edu/bioscifacpub/449>

This Article is brought to you for free and open access by the Papers in the Biological Sciences at DigitalCommons@University of Nebraska - Lincoln. It has been accepted for inclusion in Faculty Publications in the Biological Sciences by an authorized administrator of DigitalCommons@University of Nebraska - Lincoln.

Published in final edited form as:

J Nutr Biochem. 2013 August ; 24(8): 1446–1452. doi:10.1016/j.jnutbio.2012.12.003.

Holocarboxylasesynthetase interacts physically with euchromatic histone-lysine N-methyltransferase, linking histone biotinylation with methylation events*

Yong Li^{1,‡}, Yousef I. Hassan^{1,‡}, Hideaki Moriyama², and Janos Zempleni^{1,†}

¹Department of Nutrition and Health Sciences, University of Nebraska-Lincoln, NE 68583-0806, USA

²Department of Chemistry, University of Nebraska-Lincoln, NE 68583-0806, USA

Abstract

Holocarboxylasesynthetase (HCS) catalyzes the binding of the vitamin biotin to histonesH3 and H4, thereby creating rare histonebiotinylation marks in the epigenome. These marksco-localize with K9-methylated histone H3 (H3K9me), an abundant gene repression mark. The abundance of H3K9me marks in transcriptionally competent loci decreases when HCS is knocked down and when cells are depleted of biotin. Here we tested the hypothesis that the creation of H3K9me marks is at least partially explained by physical interactions between HCS and histone-lysine N-methyltransferases. Using a novel *in silico* protocol, we predicted that HCS-interacting proteins contain a GGGG(K/R)G(I/M)R motif. Thismotif, with minor variations, is present in the histone-lysine N-methyltransferase EHMT1. Physical interactions between HCS and the N-terminal, ankyrin, and SET domains in EHMT1 were confirmed using yeast-two-hybrid assays, limited proteolysis assays, and co-immunoprecipitation. The interactions were stronger between HCS and the N-terminus in EHMT1 compared with the ankyrin and SET domains, consistent with the localization of the HCS-binding motif in the EHMT1 N-terminus. HCS has the catalytic activity to biotinylate K161 within the binding motif in EHMT1. Mutation of K161 weakenedthe physical interaction between EHMT1 and HCS, but it is unknown whether this effect was caused by loss of biotinylation or loss of the motif. Importantly, HCS knockdown decreased the abundance of H3K9me marks in repeats, suggesting that HCS plays a role in creating histone methylation marks in these loci. We conclude that physical interactionsbetween HCS and EHMT1 mediate epigenomic synergies between biotinylation and methylation events.

Keywords

biotin; EHMT1; histones; holocarboxylasesynthetase; methylation

*A contribution of the University of Nebraska Agricultural Research Division, supported in part by funds provided through the Hatch Act. Additional support was provided by NIH grants DK063945, DK077816, and DK082476.

© 2012 Elsevier Inc. All rights reserved.

[†]To whom correspondence should be addressed: Janos Zempleni, Department of Nutrition and Health Sciences, University of Nebraska-Lincoln, 316C Ruth Levertton Hall, Lincoln, NE 68583-0806, USA. Fax: +1 402 472 1587., jzempleni2@unl.edu.

[‡]Contributed equally

Publisher's Disclaimer: This is a PDF file of an unedited manuscript that has been accepted for publication. As a service to our customers we are providing this early version of the manuscript. The manuscript will undergo copyediting, typesetting, and review of the resulting proof before it is published in its final citable form. Please note that during the production process errors may be discovered which could affect the content, and all legal disclaimers that apply to the journal pertain.

INTRODUCTION

Classically, holocarboxylase synthetase (HCS, EC 6.3.4.15) is appreciated for its role as a protein biotin ligase that catalyzes the covalent binding of biotin to five human carboxylases, which mediate key steps in intermediary metabolism including fatty acid synthesis, gluconeogenesis and leucine catabolism in cytoplasm and mitochondria. Recently, it was demonstrated that HCS enters nuclear structures and that HCS is a chromatin protein. Nuclear HCS is enriched in distinct loci as opposed to coating entire chromosomes. Unambiguous evidence suggests that HCS and its microbial ortholog BirA have histone biotin ligase activity. Six lysine (K) residues in histones H3 (K4, K9, and K18) and H4 (K8, K12, and K16) have been identified as targets for biotinylation by HCS, with the possibility of additional biotinylation sites in histone H2A. Biotinylated histones are overrepresented in repressed loci including pericentromeric alpha satellite repeats, long-terminal repeats, telomeres, and the promoters of the biotin transporter gene *SMVT* and the *interleukin-2* gene. Histone biotinylation might contribute toward gene repression through mediating nucleosomal condensation. Loss of histone biotinylation due to HCS knockdown and biotin depletion has been linked with severe phenotypes such as short life span and low heat resistance in *Drosophila melanogaster*, aberrant patterns of gene regulation in human cell cultures and in *Drosophila*, and de-repression of retrotransposons leading to chromosomal abnormalities. However, biotinylation of histones is a rare event and only <0.001% of histones H3 and H4 are biotinylated, raising concerns as to how the loss of such a rare event can precipitate severe phenotypes.

We hypothesized that histone biotinylation sites are primarily marks of HCS docking sites in chromatin, and that HCS and biotin contribute to gene regulation and genome stability through interactions with other chromatin proteins and epigenomic marks. This hypothesis is based on the following previous observations. (a) Erasure of cytosine methylation marks causes a substantial decrease in the abundance of histone biotinylation marks (but not vice versa). (b) Histone biotinylation marks co-localize with K9-methylated histone H3 (H3K9me), an abundant gene repression mark. (c) HCS knockdown and biotin depletion greatly diminish the abundance of H3K9me marks in distinct genomic loci. Here we developed a novel protocol for predicting HCS-binding proteins and we tested our prediction regarding the euchromatic histone-lysine N-methyltransferase EHMT1 by using a variety of molecular biology and proteomics techniques.

MATERIALS AND METHODS

Protocol for predicting HCS-interacting proteins in silico

We hypothesized that the five human carboxylases share a motif that mediates interactions with HCS and that this motif is shared by HCS-binding proteins in chromatin. Putative HCS-binding motifs in carboxylases were identified by using PROMALS multiple sequence alignment server and the following input sequences: pyruvate carboxylase (PC, gi|106049528), propionyl-CoA carboxylase (PCC, gi|65506442), acetyl-CoA carboxylase 1 (ACC 1, gi|38679960), acetyl-CoA carboxylase 2 (ACC 2, gi|134142062), and 3-methylcrotonoyl-CoA carboxylase subunit alpha (MCC α gi|116805327). Next, we selected those conserved motifs that are exposed at the carboxylase surface by modeling the 3D structures of carboxylases using Swiss-Model, 3D-JIGSAW, and Phyre. We then focused our analysis on those motifs in carboxylases that exhibited similarities in adjacent amino acids, including charge, hydrophobicity, and bulkiness. Finally, a visual inspection of 3D structures and motifs was conducted using PyMol (DeLano Scientific, San Carlos, CA) and Deep View. This procedure returned GGGG(K/R)G(I/M)R as a likely motif for mediating interactions with HCS.

ABLAST search was conducted to identify proteins containing the putative HCS-binding motif. This query identified a few putative HCS-interacting chromatin proteins including EHMT1 (truncated motif: GGAGKG), which catalyzes the methylation of K9 in histone H3. In our subsequent laboratory analyses we focused on EHMT1, because of the known synergies between histone biotinylation and H3K9me.

Yeast-two-hybrid assays

Assays were conducted as described for our previous studies using full-length HCS in vector pGBKT7 as bait. Expression of full-length human EHMT1 (GenBank accession #NM_024757.4) proved to be lethal for *E. coli* in our hands and, therefore, prey vectors were created that code for the following three EHMT1 domains, each separately cloned in vector pGADT7: N-terminal domain (M1-H611), ankyrin repeat domain (P589-A1015) and SET domain (R1002-L1298). Briefly, cDNA from HEK293 human embryonic kidney cells was PCR amplified using primers 5'-GAACATATGGCCGCCGCGGATGCCGAG-3' (forward) and 5'-CCATCGATCGGTGAGAGATGCTGCTCTCGGGC-3' (reverse) for the N-terminal domain, 5'-CCGCATATGCCTGGCTGTGGCTACTTCTGC-3' (forward) and 5'-GGGATCGATCGATGTCCCTGCTCACTATCC-3' (reverse) for the ankyrin domain, and 5'-CCCCATATGCCAGCCCCGTGGAGAGGAT-3' (forward) and 5'-GCATCGATTGTCGGGCAAGCCGTCCTCCT-3' (reverse) for the SET domain. PCR products were inserted into pGADT7 using *Nde I* and *Cla I* to produce plasmids coding for the N-terminus ("pGADT7-EHMT1N"), ankyrin repeats ("pGADT7-EHMT1A"), and SET domain ("pGADT7-EHMT1S") in human EHMT1. The identity of all plasmids was confirmed by sequencing. After transformation and mating, growth and color of yeast colonies were monitored at timed intervals for up to 14 d.

Recombinant proteins

Bioactive recombinant HCS was prepared from pET41a-HCS as described previously. For recombinant EHMT1, individual domains (N-terminus, ankyrin repeat, and SET) were PCR amplified using plasmids pGADT7-EHMT1N, pGADT7-EHMT1A, and pGADT7-EHMT1S as templates and the primers 5'-TAGGATCCATGGCCGCCGCGGATG-3' (forward) and 5'-GGGGTGCACAGGAACCAGGCTATAGGTTCCC-3' (reverse) for a truncated N-terminus (see below), 5'-CCGAATTCCTGGCTGTGGCTACTTCTGC-3' (forward) and 5'-GTCGTCGACCGATGTCCCTGCTCACTATCC-3' (reverse) for the ankyrin repeats domain, and 5'-GCGAAT TCCCCAGCCCCGTGGAGAGGAT-3' (forward) and 5'-TTGCTCGACTGTCTGGGCAAGCCGTCCTCCT-3' (reverse) for the SET domain. PCR products were ligated into the pET-28a(+) expression vector (Novagen), using *BamH I* and *SalI* to create vectors pET-28a-EHMT1N, *EcoRI* and *SalI* to create pET-28a-EHMT1A and pET-28a-EHMT1S. The identity of clones was confirmed by sequencing. Note that the full N-terminus M1-H611 did not express well and that pET-28a-EHMT1N codes only for amino acids M1-P300, a strategy necessary to achieve robust expression. EHMT1 domains were expressed in *ArcticExpress* (DE3) RP *E. coli* competent cells (Stratagene). Cells were lysed by sonication and proteins were purified using a HisTrap affinity column (GE Healthcare) and an AKTA protein purification system as described previously. The eluted sample was desalted and concentrated using 5kD Spin-X UF concentrator (Corning). Molecular weight and integrity of His-tagged EHMT1 proteins were confirmed using gel electrophoresis (NuPAGE 4–12% Bis-Tris gel, Invitrogen) and coomassie blue staining.

Deletions and mutations in the truncated EHMT1 N-terminus were created using the Gene Tailor™ Site-Directed Mutagenesis System (Invitrogen). Using plasmid pET-28a-EHMT1N as template, we used primers 5'-CCCTTCTGGAGGGGCTGGCAGAGGCAGGACTCC-3' (forward) and 5'-GCCAGCCCCTCCAGGAAGGGTTTTGCAGC-3' (reverse) for creating a K161R

mutant (“pET-28a-EHMT1N_{K161R}”), and primers 5′-GCTGCAAAACCCCTTCCTAGGACTCCAAGCG-3′ (forward) and 5′-AGGAAGGGTTTTTGCAGCATGGCCAGGCAG-3′ (reverse) for creating a GGAGKG deletion mutant (“pET-28a-EHMT1N_{del}”). The identities of mutant plasmids were confirmed by sequencing.

Limited proteolysis assays

Limited proteolysis assays were conducted as described previously, using equal molar mixtures of recombinant HCS and EHMT1. Samples were collected 5, 10 and 30 min after initiation of digestion with 10 ng trypsin per μ g of recombinant protein; baseline controls were collected before addition of trypsin. Proteolytic digestion of EHMT1 and HCS was assessed by gel electrophoresis and staining with coomassie blue.

Biotinylation of EHMT1 domains by HCS

We tested whether recombinant human EHMT1 is a target for biotinylation by HCS. Briefly, the three domains in recombinant EHMT1 were incubated with full-length HCS, biotin, and cofactors. Proteins were resolved on NuPAGE 4–12% Bis-Tris gels and EHMT1-bound biotin was probed using IRDye® 800CW streptavidin (LI-COR; Lincoln, NE) and an Odyssey infrared imaging system (LI-COR).

Co-immunoprecipitation assays

Full-length human Flag-tagged EHMT1 was obtained from Dr. Jiandong Chen, Department of Molecular Oncology, Moffitt Cancer Center; Tampa FL. HCS was subcloned from pGBKT7-HCS into the pCMV-Myc plasmid with *Sfi*I and *Sal*I to create plasmid pCMV-Myc-HCS. Individual domains of EHMT1 were subcloned from pGADT7-EHMT1N by using 5′-TTTGTGACATGGCCGCCGCGATGCCGAG-3′ (forward primer), 5′-GGCGGTACCCGGTGAGAGATGCTGCTCTCGGGC-3′ (reverse primer), and *Sal*I and *Kpn*I, from pGADT7-EHMT1A by using 5′-CCGAATTCGTCTGGCTGTGGCTACTTCTGC-3′ (forward primer), 5′-GTCGTCGACCGATGTCCCTGCTCACTATCC-3′ (reverse primer), and *Eco*RI and *Sal*I, and from pGADT7-EHMT1S by using 5′-GCGAATTCGGCCAGCCCCGTGGAGAGGAT-3′ (forward primer), 5′-TTCGTCGACTGTCGGGCAAGCCGTCCTCCT-3′ (reverse primer), and *Eco*RI and *Sal*I into the pCMV-HA vector to create plasmids pCMV-HA-EHMT1N, pCMV-HA-EHMT1A, and pCMV-HA-EHMT1S, respectively. The identity of all plasmids was confirmed by sequencing. Plasmids were isolated using the Maxi Prep Kit (Qiagen) for co-transfection into HEK293 cells using Lipofectamine 2000 reagent (Invitrogen). Twenty-four hours after transfection, cells were lysed using non-denaturing lysis buffer (20mM TrisHCl, pH8, 137mM NaCl, 10% Glycerol, 1% Triton X100, and 2mM EDTA). Co-immunoprecipitation assay was conducted as described to assess the interactions between myc-tagged HCS and Flag-tagged full-length EHMT1 or HA-tagged EHMT1 domains. Tagged proteins were precipitated using anti-HA and anti-Flag (Abcam); proteins in the precipitate were resolved using NuPAGE 4–12% Bis-Tris gels and probed with monoclonal anti-myc (OriGene) and anti-HCS serum.

HCS knockdown cells

HCS was transiently knocked down by transfecting 2×10^6 HEK293 cells with 2nM of HCS Trilencer-27 Human siRNA (OriGene) using Lipofectamine 2000 (Invitrogen). Controls were transfected with siRNA not targeting any human gene (Negative Control siRNA, OriGene). Cells were collected 3 d after transfection. Knockdown was confirmed using quantitative real-time PCR and by western blot analysis. Proteins were resolved using 3–8%

Tris-Acetate gels (Invitrogen) and transblots were probed with anti-HCS serum using IRDye® 800CW anti-rabbit IgG (LI-COR) and an Odyssey infrared imaging system.

Chromatin immunoprecipitation assays

Chromatin immunoprecipitation assays were used to quantify the enrichment of H3K9me2 (ab7312; Abcam) in pericentromeric alpha satellite repeats (Chr4alpha), long terminal repeats (LTR15), and Glyceraldehyde-3-phosphate dehydrogenase (GAPDH, euchromatin control) as described.

Statistics

Student's t test was used to test for the statistical significance of effects. StatView 5.0.1 (SAS Institute) was used to perform all calculations. Differences were considered significant if $P < 0.05$. Data are expressed as means \pm S.D.

RESULTS

In silico prediction of HCS-binding proteins

The search for HCS-binding motifs and subsequent *in silico* modeling returned two possible consensus motifs for mediating physical interactions with HCS (Fig. 1, motifs highlighted in blue and green). We focused on the GGGG(K/R)G(I/M)R motif in our subsequent studies because that motif is exposed on the surface of known HCS-interacting proteins such as human ACC1, whereas the other motif is buried inside the proteins (Figs. 1A and 1B). The protrusion of K365 in ACC1 is particularly noteworthy. This glycine rich sequence adjacent to the lysine residue resembles the ATP binding motif in various carboxylases.

We searched the NCBI human reference protein database using position-specific iterated BLAST (PSI-BLAST) for the GGGG(K/R)G(I/M)R motif. Our query returned two proteins that play a role in gene repression through epigenetic mechanisms, namely EHMT1 and the nuclear receptor co-repressor 2 (N-CoR2). A truncated variation of the GGGG(K/R)G(I/M)R motif resides in the N-terminus (G157-R164) of EHMT1 (sequence GGAGKG) and near the C-terminus of N-CoR2. Here we focused on EHMT1 because of the well-established links among HCS, biotin, and methylation of histones. The physical interactions and synergies between HCS and N-CoR2 are investigated in a separate study.

HCS/EHMT1 interactions in yeast-two-hybrid assays

Yeast-two-hybrid assays produced results consistent with physical interactions between full-length HCS and the N-terminus, ankyrin domain, and SET domain in EHMT1 (Fig. 2). When yeast strain AH109 was transformed with pGBKT7-HCS (bait), and yeast strain Y187 was transformed with the individual EHMT1 domains in vector pGADT7 (prey), mated yeast produced blue colonies on SD/-Leu/-Trp/X- α -Gal plates within 7 days at 30°C. The growth of blue colonies is a marker for diploid yeast expressing the α -galactosidase MEL1 due to bait/prey interactions. As a positive control, we mated pGADT7-p53 with pGBKT7-T-antigen, which produced a strong blue signal. Negative controls in which empty vectors pGBKT7 and pGADT7 were substituted for pGBKT7-HCS and pGADT7-EHMT1 domains, respectively, produced no blue color. Note that white colonies are controls for mating efficiency, but do not select for bait/prey interactions. In previous studies we have demonstrated that HCS interacts physically with a fragment of the biotin-dependent propionyl-CoA carboxylase, which is considered a positive control. Yeast-two-hybrid assays tend to produce false positives and we confirmed our findings by the additional, independent assays described below.

HCS/EHMT1 interactions in co-immunoprecipitation assays

Co-immunoprecipitation assays produced results consistent with physical interactions between HCS and EHMT1. First, we transfected HEK293 cells with full-length Flag-tagged EHMT1 and an empty pCMV-Myc vector, and confirmed expression of EHMT1 by using anti-Flag (Fig. 3A); myc is small and ran off the gel. As expected, when lysates were precipitated with anti-Flag and probed with anti-myc, no signal was detectable in this negative control sample. In contrast, when myc-tagged HCS and full-length Flag-tagged EHMT1 were co-expressed, both proteins were detectable in input material probed with anti-myc and anti-Flag, respectively. When EHMT1 in this sample was precipitated with anti-Flag, we detected a strong HCS signal in the precipitate when anti-myc was used as probe. Mutations and deletions in the GGAGKG variant motif in EHMT1 impaired the interactions with HCS. We substituted EHMT1 constructs containing either a point mutation or a deletion for wild-type EHMT1 and repeated our overexpression and co-immunoprecipitation experiments. In the point mutant, we substituted an arginine for the lysine in the GGAGKG motif, and in the deletion construct we deleted the entire GGAGKG motif. Both constructs expressed well in HEK293, but the co-immunoprecipitation of myc-tagged HCS for the two mutants was less efficient than that seen for the wild-type sequence.

Next, we assessed the interactions of individual EHMT1 domains with HCS. We co-expressed full-length myc-tagged HCS with the HA-tagged N-terminus, ankyrin repeats domain, and SET domain in HEK293 cells; controls were transfected with empty vectors. Expression of tagged proteins was confirmed using anti-myc and anti-HA (Fig. 3B, upper two “input” gels). HA-tagged EHMT1 fusion constructs in protein lysates were precipitated with anti-HA, and the precipitated proteins were probed with anti-myc and anti-HCS. Both probes produced a strong signal, suggesting that EHMT1 interacts physically with HCS. The signal strength was N-terminus > ankyrin repeats domain > SET domain, particularly if considering that the SET construct expressed better than the other two EHMT1 domains (compare “input gels”). It is not surprising that N-terminus and ankyrin domain produced stronger signals than the SET domain, because the HCS-interacting motif resides in the N-terminus, and because ankyrin repeats are known to mediate protein/protein interactions.

HCS/EHMT1 interactions in limited proteolysis assays

Limited proteolysis assays produced results consistent with a physical interaction between EHMT1 and HCS. First, recombinant EHMT1 and HCS were expressed and purified as substrates for these assays. The expression of full-length EHMT1 proved to be lethal for *Escherichia coli* and, therefore, we sought to express individual domains. Ankyrin and SET domain expressed and purified well, but we did not succeed in obtaining the N-terminal domain (M1-H611). Therefore, we truncated the N-terminus to express M1-P300, which includes the GGAGKG variant motif, for subsequent limited proteolysis assays.

When HCS was incubated with the various EHMT1 domains prior to tryptic digestion, the rate of HCS degradation was slowed compared with HCS treated in the absence of EHMT1 (Fig. 4). Consistent with the results seen in the co-immunoprecipitation assays, limited proteolysis assays also suggest that the N-terminus and the ankyrin repeats domain in EHMT1 interact stronger than the SET domain with HCS.

Biotinylation of EHMT1 domain by HCS

Lysine residues in EHMT1 are targets for biotinylation by HCS. EHMT1 contains multiple lysine residues including a lysine in the HCS-binding motif GGGG(K/R)G(I/M)R, which equals K161 within the GGAGKG variant motif in full-length EHMT1. When recombinant EHMT1 domains were incubated with HCS, biotin, and cofactors, we observed a time-dependent increase in the biotinylation signal in the N-terminus, ankyrin repeats domain, and

the SET domain of EHMT1 (Fig. 5A). The signal was stronger in the N-terminus compared with the other domains; equal loading was confirmed by staining with coomassie blue. K161 in EHMT1 appears to be a preferred target for biotinylation by HCS. When K161 was deleted by site-directed mutagenesis, the biotinylation signal decreased considerably compared with the wild-type N-terminus (Fig. 5B). Likewise, the signal decreased considerably when the entire HCS-binding motif was deleted. The magnitude of the effect reached up to 48% less biotinylation compared with wild-type, depending on time point and mutant (Fig. 5C).

Mutation of K161 and deletion of the GGAGKG motif weaken the physical interactions between HCS and EHMT1. When the EHMT1_{N_{K161R}} point mutant and the EHMT1_{N_{del}} construct were tested in limited proteolysis assays, the rate of HCS degradation was considerably accelerated in mutant and deletion construct compared with the wild-type N-terminus of EHMT1 (Fig. 6). While it is tempting to speculate that biotinylation of K161 in EHMT1 is a crucial event in strengthening the interaction between HCS and EHMT1, we acknowledge that the loss of biotinylation may be coincidental and that the entire effect is caused by the deletion or alteration of the HCS-interacting motif.

Effects of HCS knockdown on the abundance of H3K9me2 marks

HCS knockdown causes a decrease of H3K9me2 marks in pericentromeric alpha satellite repeats in chromosome 4 and in LTR15 in HEK293 cells compared with cells treated with a control siRNA (Fig. 7A). The decrease amounted to a 50% lower abundance of H3K9me2 marks in HCS knockdown cells compared to negative controls.

Successful knockdown of HCS was confirmed by western blot analysis (Fig. 7B), using pyruvate carboxylase and histone H4 as loading controls, and by quantitative real-time PCR (Fig. 7C), using GAPDH for normalization of PCR efficacy. Both western blot analysis and PCR suggested that the expression of HCS was knocked down by 64% compared with negative control sample. Importantly, the western blots suggest that the global abundance of H3K9me2 in bulk extracts of histones was not altered by HCS knockdown (Fig. 7B), i.e., that the decrease of H3K9me2 in repeat regions is locus-specific. Also, the real-time PCR studies suggest that HCS knockdown does not affect the expression of EHMT1 (Fig. 7C). Previous studies suggest that the expression of histone H3 does not depend on biotin or HCS.

DISCUSSION

This is the first report describing physical interactions between the histone-biotin ligase HCS and the histone-lysine methyltransferase EHMT1. The confidence level is high that this interaction is real, based on the following lines of reasoning. (a) Interactions were predicted using a novel *in silico* protocol that identified an HLCS-binding motif in EHMT1. (b) Predictions were validated in the laboratory using three distinct procedures, namely yeast-two-hybrid assays, limited proteolysis assays, and co-immunoprecipitation assays. (c) Interactions between HCS and EHMT1 were weakened when the HCS-binding motif was experimentally altered by site-directed mutagenesis or deletion. (d) HCS interacts stronger with the N-terminus in EHMT1, which contains the new HCS-binding motif, and with the ankyrin repeats domain in EHMT1, which is known to be important for mediating protein/protein interactions, than with the SET domain in EHMT1. (e) HCS catalyzes the biotinylation of K161 and other lysines in EHMT1.

Importantly, the interaction is biologically meaningful because HCS knockdown caused a decrease in the enrichment of H3K9me2 marks in pericentromeric alpha satellite repeats and LTRs. H3K9me2 is a gene repression marker and we have reported previously that biotin

and HCS depletion causes a de-repression of LTRs in metazoans that coincides with a depletion of H3K9me2 marks. In these previous studies, the de-repression of LTRs was associated with a 300% increase in retrotransposition events in *Drosophila* and with 0.7 gross chromosomal abnormalities per metaphase cell in biotin-depleted human cell cultures compared to zero abnormalities in biotin-sufficient and biotin-supplemented cultures. LTRs pose a burden to genome stability, as their mobilization facilitates recombination between non-homologous loci, leading to chromosomal deletions and translocations. It is noteworthy that the human genome contains about 60 fully functional LTRs that are capable of initiating retrotransposition events. Posttranslational modifications of histones and methylation of cytosine residues in DNA are among the well-established mechanisms to repress retrotransposons.

What are the uncertainties remaining? First, we do not know whether the HCS-dependent biotinylation of EHMT1 is biologically important *in vivo*. In ongoing mass spectrometry studies we failed to detect biotinylated EHMT1 even after enriching for biotinylated proteins (unpublished observation), suggesting that biotinylation of EHMT1 might be a rare event *in vivo*. However, our biotinylation studies with recombinant HCS and EHMT1 provide unambiguous evidence that HCS has the catalytic activity to biotinylate EHMT1. Also, previous studies with synthetic lysine-containing peptides suggest that HCS does not arbitrarily catalyze biotinylation of any lysine residue in HCS-interacting proteins. Second, we failed to detect a change in the global abundance of H3K9me2 in cell extracts in HCS knockdown cells, whereas the local enrichment of the mark decreased in repeat regions Chr4alpha and LTR15. The human genome encodes for H3K9 methyltransferases other than EHMT1, e.g., SETDB1 and ESET. Histone methyl transferases other than EHMT1 may not interact with HCS. It remains to be determined whether this redundancy of methyltransferases causes the lack of effect of HCS knockdown on the abundance of H3K9me marks in whole cell extracts of histones. This issue will need to be addressed in future studies demonstrating co-localization of HCS and EHMT1 in the same loci by using chromatin immunoprecipitation studies, or by using transgenic cell lines in which histone methyl transferases other than EHMT1 have been knocked down. Third, the *in silico* protocol for predicting HCS-binding proteins suggests that N-CoR2 also interacts with HCS. We are currently testing this prediction and initial results look promising. Fourth, the HCS-binding motif in EHMT1 (GGAGKG) is not a perfect match for the predicted motif [GGGG(K/R)G(I/M)R] and it remains to be seen how many HCS-interacting proteins can be identified in future studies allowing for the use of a more degenerate motif.

We conclude that HCS exerts some of its roles in gene regulation through the formation of multiprotein gene repression complexes in human chromatin. Possible members of this complex include proteins involved in DNA methylation, EHMT1, and N-CoR2. Because of the role of N-CoR in recruiting histone deacetylases, it seems reasonable that histone deacetylases are also part of the proposed multiprotein complex. This theory would integrate previous observations that HCS and biotin are important for gene repression, the low abundance of biotinylated histones in chromatin, and the known roles of members of the putative multiprotein complex in mediating gene repression into a coherent model.

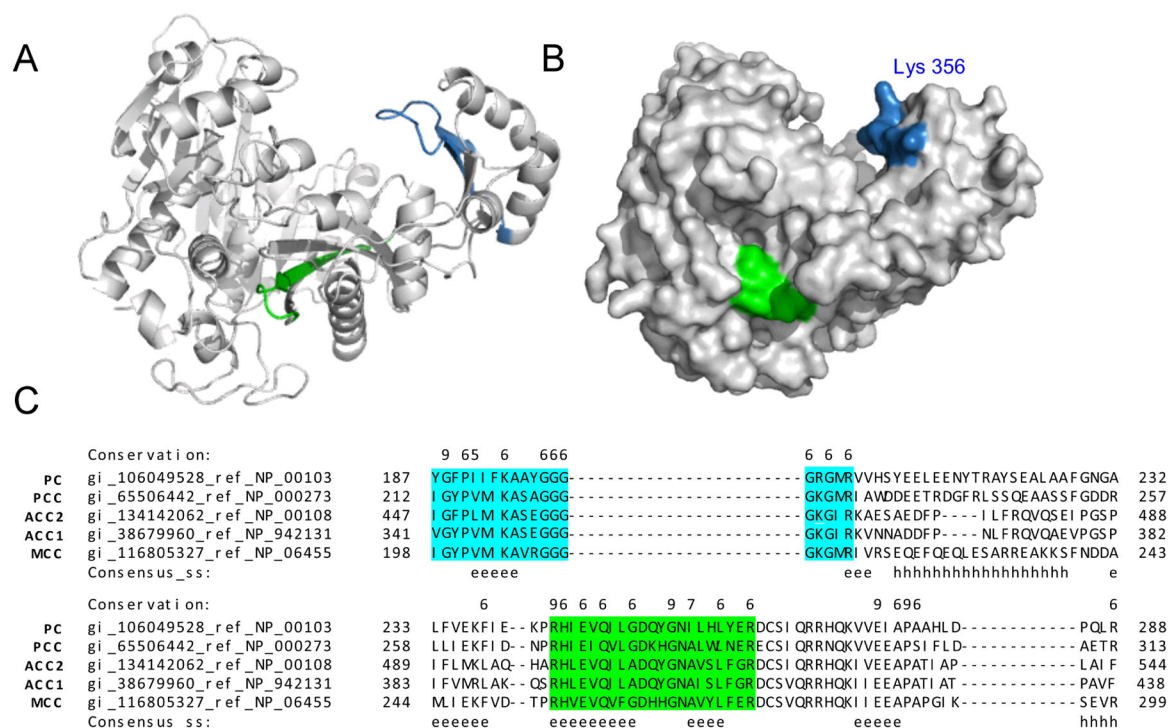
References

1. Suzuki Y, Aoki Y, Ishida Y, Chiba Y, Iwamatsu A, Kishino T, et al. Isolation and characterization of mutations in the human holocarboxylase synthetase cDNA. *Nat Genet.* 1994; 8:122–28. [PubMed: 7842009]
2. Zemleni J, Wijeratne SS, Hassan YI. Biotin. *BioFactors* (Oxford, England). 2009; 35:36–46.

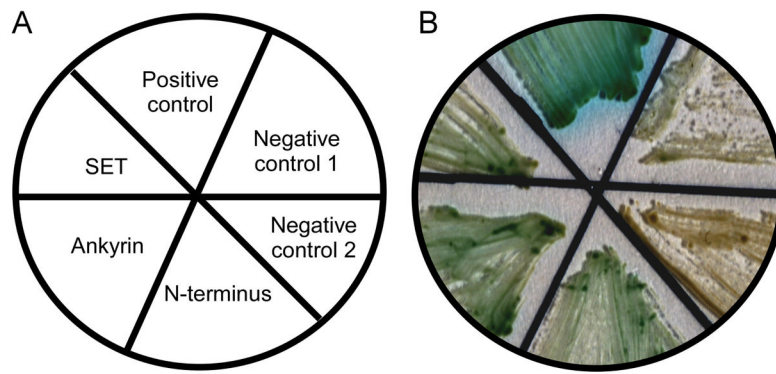
3. Narang MA, Dumas R, Ayer LM, Gravel RA. Reduced histone biotinylation in multiple carboxylase deficiency patients: a nuclear role for holocarboxylasesynthetase. *Hum Mol Genet.* 2004; 13:15–23. [PubMed: 14613969]
4. Chew YC, Camporeale G, Kothapalli N, Sarath G, Zempleni J. Lysine residues in N- and C-terminal regions of human histone H2A are targets for biotinylation by biotinidase. *J NutrBiochem.* 2006; 17:225–33.
5. Bailey LM, Wallace JC, Polyak SW. Holocarboxylasesynthetase: correlation of protein localisation with biological function. *Arch BiochemBiophys.* 2010; 496:45–52.
6. Bao B, Wijeratne SS, Rodriguez-Melendez R, Zempleni J. Human holocarboxylasesynthetase with a start site at methionine-58 is the predominant nuclear variant of this protein and has catalytic activity. *BiochemBiophys Res Commun.* 2011; 412:115–20.
7. Camporeale G, Giordano E, Rendina R, Zempleni J, Eissenberg JC. *Drosophila* holocarboxylasesynthetase is a chromosomal protein required for normal histone biotinylation, gene transcription patterns, lifespan and heat tolerance. *J Nutr.* 2006; 136:2735–42. [PubMed: 17056793]
8. Singh D, Pannier AK, Zempleni J. Identification of holocarboxylasesynthetase chromatin binding sites using the DamID technology. *Anal Biochem.* 2011; 413:55–59. [PubMed: 21303649]
9. Kobza K, Camporeale G, Rueckert B, Kueh A, Griffin JB, Sarath G, et al. K4, K9, and K18 in human histone H3 are targets for biotinylation by biotinidase. *FEBS J.* 2005; 272:4249–59. [PubMed: 16098205]
10. Bao B, Pestinger V, IHY, Borgstahl GEO, Kolar C, Zempleni J. Holocarboxylasesynthetase is a chromatin protein and interacts directly with histone H3 to mediate biotinylation of K9 and K18. *J NutrBiochem.* 2011; 22:470–75.
11. Stanley JS, Griffin JB, Zempleni J. Biotinylation of histones in human cells: effects of cell proliferation. *Eur J Biochem.* 2001; 268:5424–29. [PubMed: 11606205]
12. Camporeale G, Shubert EE, Sarath G, Cerny R, Zempleni J. K8 and K12 are biotinylated in human histone H4. *Eur J Biochem.* 2004; 271:2257–63. [PubMed: 15153116]
13. Camporeale G, Oommen AM, Griffin JB, Sarath G, Zempleni J. K12-biotinylated histone H4 marks heterochromatin in human lymphoblastoma cells. *J NutrBiochem.* 2007; 18:760–68.
14. Kuroishi T, Rios-Avila L, Pestinger V, Wijeratne SS, Zempleni J. Biotinylation is a natural, albeit rare, modification of human histones. *Mol Genet Metab.* 2011; 104:537–45. [PubMed: 21930408]
15. Pestinger V, Wijeratne SSK, Rodriguez-Melendez R, Zempleni J. Novel histone biotinylation marks are enriched in repeat regions and participate in repression of transcriptionally competent genes. *J NutrBiochem.* 2011; 22:328–33.
16. Rios-Avila L, Pestinger V, Zempleni J. K16-biotinylated histone H4 is overrepresented in repeat regions and participates in the repression of transcriptionally competent genes in human Jurkat lymphoid cells. *J NutrBiochem.* 2012; 23:1559–64.
17. Chew YC, West JT, Kratzer SJ, Ilvarsonn AM, Eissenberg JC, Dave BJ, et al. Biotinylation of histones represses transposable elements in human and mouse cells and cell lines, and in *Drosophila melanogaster*. *J Nutr.* 2008; 138:2316–22. [PubMed: 19022951]
18. Gralla M, Camporeale G, Zempleni J. Holocarboxylasesynthetase regulates expression of biotin transporters by chromatin remodeling events at the SMVT locus. *J NutrBiochem.* 2008; 19:400–08.
19. Wijeratne SS, Camporeale G, Zempleni J. K12-biotinylated histone H4 is enriched in telomeric repeats from human lung IMR-90 fibroblasts. *J NutrBiochem.* 2010; 21:310–16.
20. Filenko NA, Kolar C, West JT, Hassan YI, Borgstahl GEO, Zempleni J, et al. The role of histone H4 biotinylation in the structure and dynamics of nucleosomes. *PLoS ONE.* 2011; 6:e16299. [PubMed: 21298003]
21. Bailey LM, Ivanov RA, Wallace JC, Polyak SW. Artifactual detection of biotin on histones by streptavidin. *Anal Biochem.* 2008; 373:71–77. [PubMed: 17920026]
22. Kouzarides, T.; Berger, SL. Chromatin modifications and their mechanism of action. In: Allis, CD.; Jenuwein, T.; Reinberg, D., editors. *Epigenetics*. Cold Spring Harbor Press; Cold Spring Harbor, NY: 2007. p. 191-209.
23. Pei J, Grishin NV. PROMALS: towards accurate multiple sequence alignments of distantly related proteins. *Bioinformatics.* 2007; 23:802–8. [PubMed: 17267437]

24. Arnold K, Bordoli L, Kopp J, Schwede T. The SWISS-MODEL workspace: a web-based environment for protein structure homology modelling. *Bioinformatics*. 2006; 22:195–201. [PubMed: 16301204]
25. Contreras-Moreira B, Bates PA. Domain fishing: a first step in protein comparative modelling. *Bioinformatics*. 2002; 18:1141–2. [PubMed: 12176841]
26. Kelley LA, Sternberg MJ. Protein structure prediction on the Web: a case study using the Phyre server. *Nature protocols*. 2009; 4:363–71.
27. Guex N, Peitsch MC. SWISS-MODEL and the Swiss-PdbViewer: an environment for comparative protein modeling. *Electrophoresis*. 1997; 18:2714–23. [PubMed: 9504803]
28. Altschul SF, Gish W, Miller W, Myers EW, Lipman DJ. Basic local alignment search tool. *J MolBiol*. 1990; 215:403–10.
29. Ogawa H, Ishiguro K, Gaubatz S, Livingston DM, Nakatani Y. A complex with chromatin modifiers that occupies E2F- and Myc-responsive genes in G0 cells. *Science*. 2002; 296:1132–6. [PubMed: 12004135]
30. Hassan YI, Moriyama H, Olsen LJ, Bi X, Zemleni J. N- and C-terminal domains in human holocarboxylasesynthetase participate in substrate recognition. *Mol Genet Metab*. 2009; 96:183–88. [PubMed: 19157941]
31. Fontana A, de Laureto PP, Spolaore B, Frare E, Picotti P, Zamboni M. Probing protein structure by limited proteolysis. *ActaBiochim Pol*. 2004; 51:299–321.
32. Leon-Del-Rio A, Gravel RA. Sequence requirements for the biotinylation of carboxyl-terminal fragments of human propionyl-CoA carboxylase alpha subunit expressed in *Escherichia coli*. *Journal of Biological Chemistry*. 1994; 269:22964–68. [PubMed: 8083196]
33. Bonifacino JS, Dell'Angelica EC, Springer TA. Immunoprecipitation. *CurrProtocImmunol*. 2001; Chapter 8(Unit 8):3.
34. Kaur Mall G, Chew YC, Zemleni J. Biotin requirements are lower in human Jurkat lymphoid cells but homeostatic mechanisms are similar to those of HepG2 liver cells. *J Nutr*. 2010; 140:1086–92. [PubMed: 20357078]
35. Kwon K, Beckett D. Function of a conserved sequence motif in biotin holoenzymesynthetases. *Protein Sci*. 2000; 9:1530–9. [PubMed: 10975574]
36. Li J, Mahajan A, Tsai MD. Ankyrin repeat: a unique motif mediating protein-protein interactions. *Biochemistry*. 2006; 45:15168–78. [PubMed: 17176038]
37. Mosavi LK, Cammett TJ, Desrosiers DC, Peng ZY. The ankyrin repeat as molecular architecture for protein recognition. *Protein Sci*. 2004; 13:1435–48. [PubMed: 15152081]
38. Kazazian HH Jr, Moran JV. The impact of L1 retrotransposons on the human genome. *Nat Genet*. 1998; 19:19–24. [PubMed: 9590283]
39. Kazazian HH Jr. Mobile elements: drivers of genome evolution. *Science*. 2004; 303:1626–32. [PubMed: 15016989]
40. Buzdin A. Human-specific endogenous retroviruses. *Scientific World Journal*. 2007; 7:1848–68. [PubMed: 18060323]
41. Martens JH, O'Sullivan RJ, Braunschweig U, Opravil S, Radolf M, Steinlein P, et al. The profile of repeat-associated histone lysine methylation states in the mouse epigenome. *EMBO J*. 2005; 24:800–12. [PubMed: 15678104]
42. Jaenisch R, Schnieke A, Harbers K. Treatment of mice with 5-azacytidine efficiently activates silent retroviral genomes in different tissues. *ProcNatlAcadSci USA*. 1985; 82:1451–55.
43. Jahner D, Stuhlmann H, Stewart CL, Harbers K, Lohler J, Simon I, et al. De novo methylation and expression of retroviral genomes during mouse embryogenesis. *Nature*. 1982; 298:623–28. [PubMed: 6285203]
44. Stewart CL, Stuhlmann H, Jahner D, Jaenisch R. De novo methylation, expression, and infectivity of retroviral genomes introduced into embryonal carcinoma cells. *ProcNatlAcadSci USA*. 1982; 79:4098–102.
45. Lengauer C, Kinzler KW, Vogelstein B. DNA methylation and genetic instability in colorectal cancer cells. *ProcNatlAcadSci USA*. 1997; 94:2545–50.

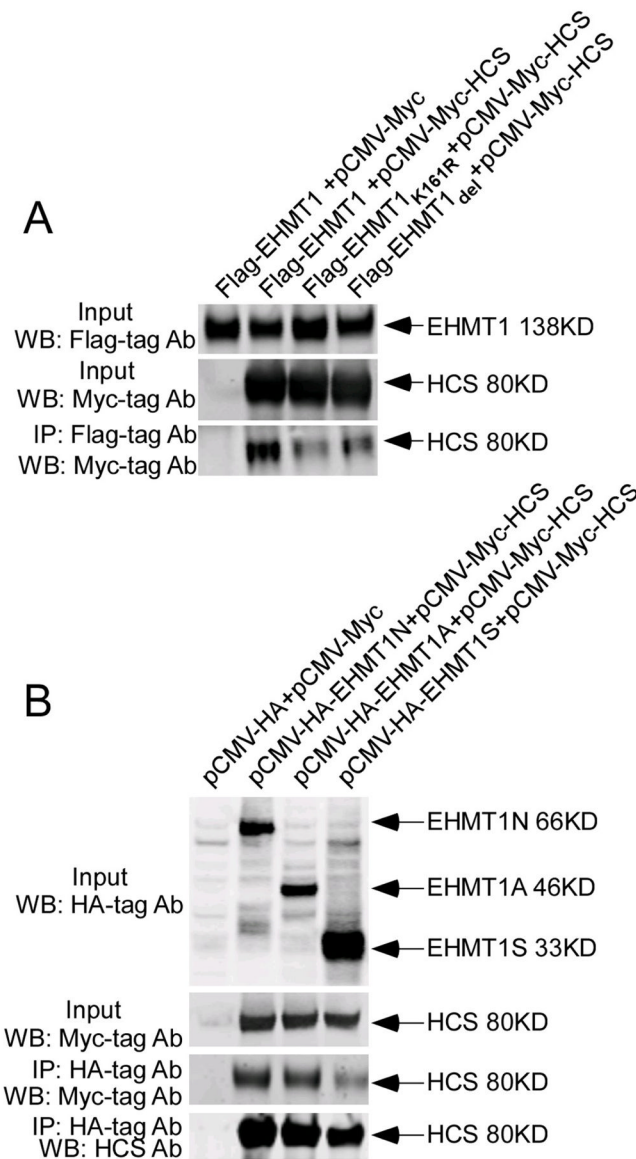
46. Lengauer C, Kinzler KW, Vogelstein B. Genetic instabilities in human cancers. *Nature*. 1998; 396:643–49. [PubMed: 9872311]
47. Eden A, Gaudet F, Waghmare A, Jaenisch R. Chromosomal instability and tumors promoted by DNA hypomethylation. *Science*. 2003; 300:455. [PubMed: 12702868]
48. Gaudet F, Hodgson JG, Eden A, Jackson-Grusby L, Dausman J, Gray JW, Leonhardt H, Jaenisch R. Induction of tumors in mice by genomic hypomethylation. *Science*. 2003; 300:489–92. [PubMed: 12702876]
49. Hassan YI, Moriyama H, Zemleni J. The polypeptide Syn67 interacts physically with human holocarboxylasesynthetase, but is not a target for biotinylation. *Arch BiochemBiophys*. 2009; 495:35–41.
50. Schultz DC, Ayyanathan K, Negorev D, Maul GG, Rauscher FJ 3rd. SETDB1: a novel KAP-1-associated histone H3, lysine 9-specific methyltransferase that contributes to HP1-mediated silencing of euchromatic genes by KRAB zinc-finger proteins. *Genes Dev*. 2002; 16:919–32. [PubMed: 11959841]
51. Yang L, Xia L, Wu DY, Wang H, Chansky HA, Schubach WH, Hickstein DD, Zhang Y. Molecular cloning of ESET, a novel histone H3-specific methyltransferase that interacts with ERG transcription factor. *Oncogene*. 2002; 21:148–52. [PubMed: 11791185]

**Fig 1.**

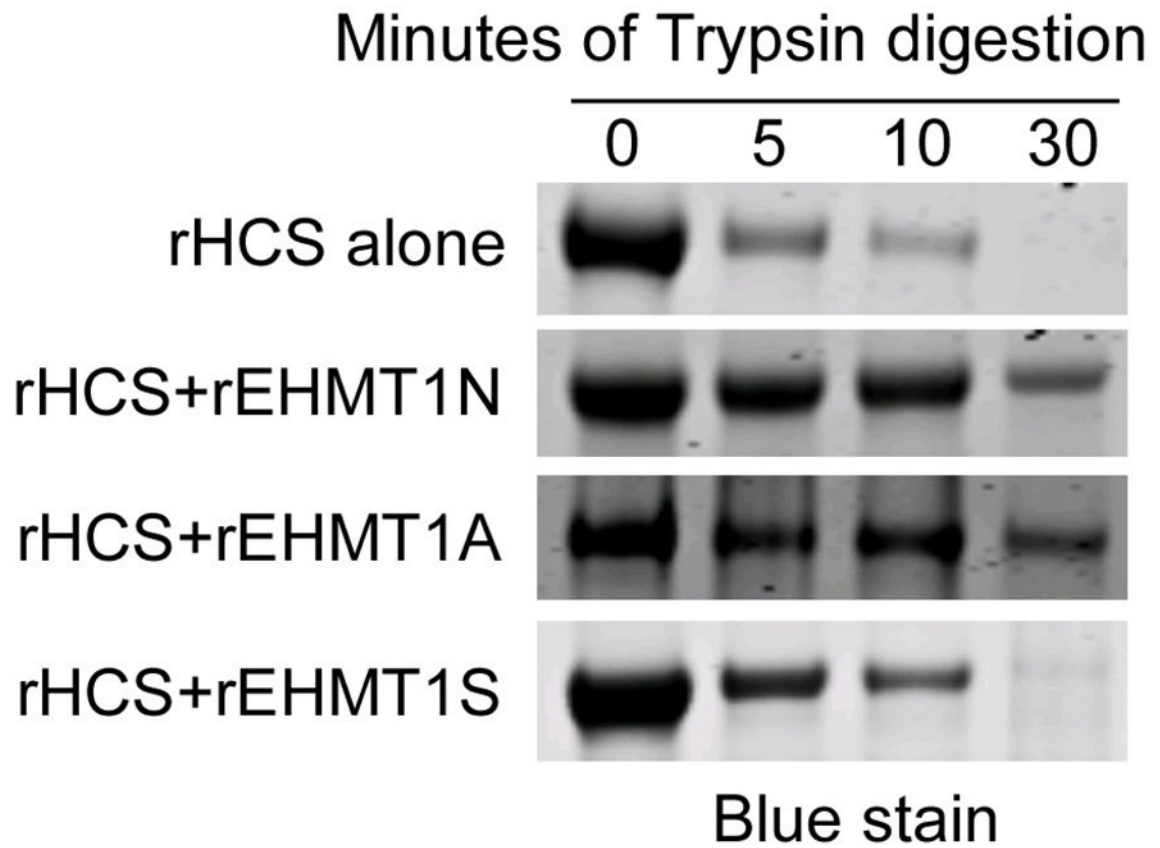
Structure of monomeric human acetyl-CoA carboxylase 1 in cartoon (A) and molecular surface (B) representation. Putative HCS-interacting domains are highlighted in blue and green, and the protrusion of K365 at the molecule surface is marked. (C) Sequence alignments of human carboxylases reveal potential HCS-interacting motifs, which are highlighted in blue and green.

**Fig 2.**

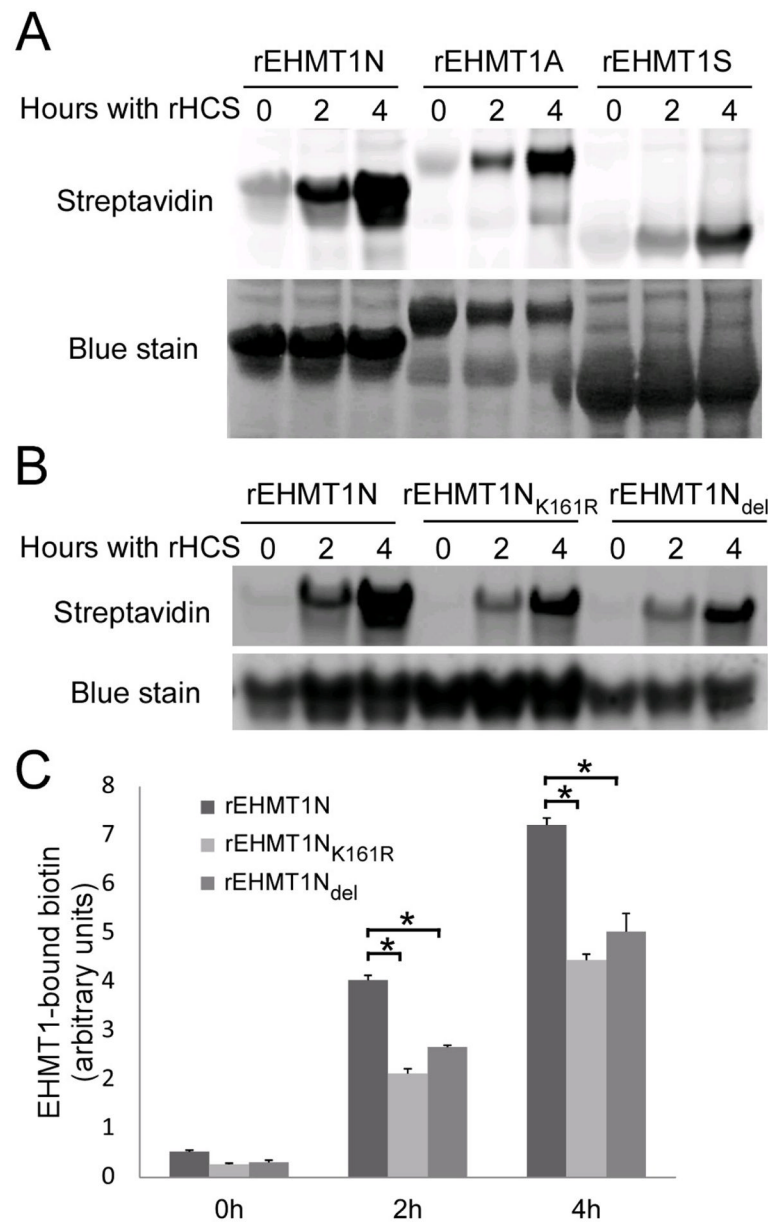
The N-terminal domain, ankyrin repeat domain, and SET domain in EHMT1 interact with human HCS in yeast-two-hybrid assays. (A) Plate layout: N-terminus = pGADT7-EHMT1N mated with pGBKT7-HCS; ankyrin = pGADT7-EHMT1A mated with pGBKT7-HCS; SET = pGADT7-EHMT1S mated with pGBKT7-HCS; positive control = pGADT7-p53 mated with pGBKT7-T-antigen; negative control 1 = mixture of pGADT7-EHMT1N, pGADT7-EHMT1A, and pGADT7-EHMT1S mated with pGBKT7; negative control 2 = pGADT7 mated with pGBKT7-HCS. (B) Growth of colonies and activation of the α -galactosidase (MEL1) reporter gene on a SD/-Leu, -Trp/X- α -gal plate seven days after mating.

**Fig 3.**

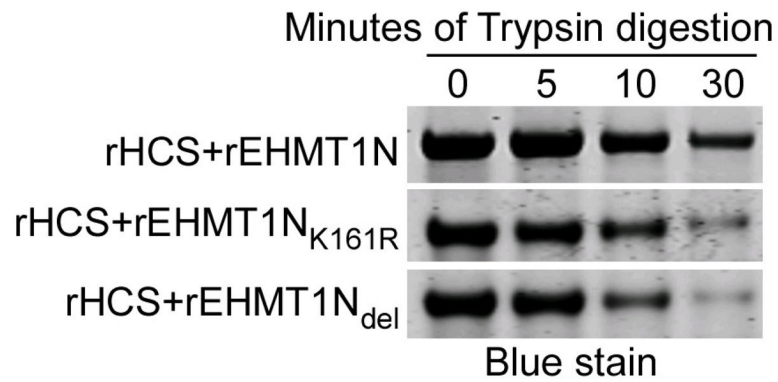
HCS interacts with EHMT1 in co-immunoprecipitation assays in HEK293 cells. (A) Flag-tagged EHMT1, a K161R point mutant, and a GGAGKG deletion mutant were co-expressed with full-length, myc-tagged HCS or empty pCMV-Myc vector. Expression was confirmed in input material by western blot analysis, using anti-Flag and anti-myc as probes. EHMT1 in lysate was precipitated using anti-Flag, and HCS in the precipitated material was probed using anti-myc. (B) HA-tagged domains in EHMT1 were co-expressed with myc-tagged full-length HCS; control cells were prepared by using empty pCMV-HA and pCMV-Myc vectors. Expression of EHMT1 constructs and HCS was confirmed in input material by western blot analysis, using anti-HA and anti-myc as probes. EHMT1 in lysate was precipitated using anti-HA, and HCS in the precipitated material was probed using anti-myc and anti-HCS. Abbreviation: IP = immunoprecipitation.

**Fig 4.**

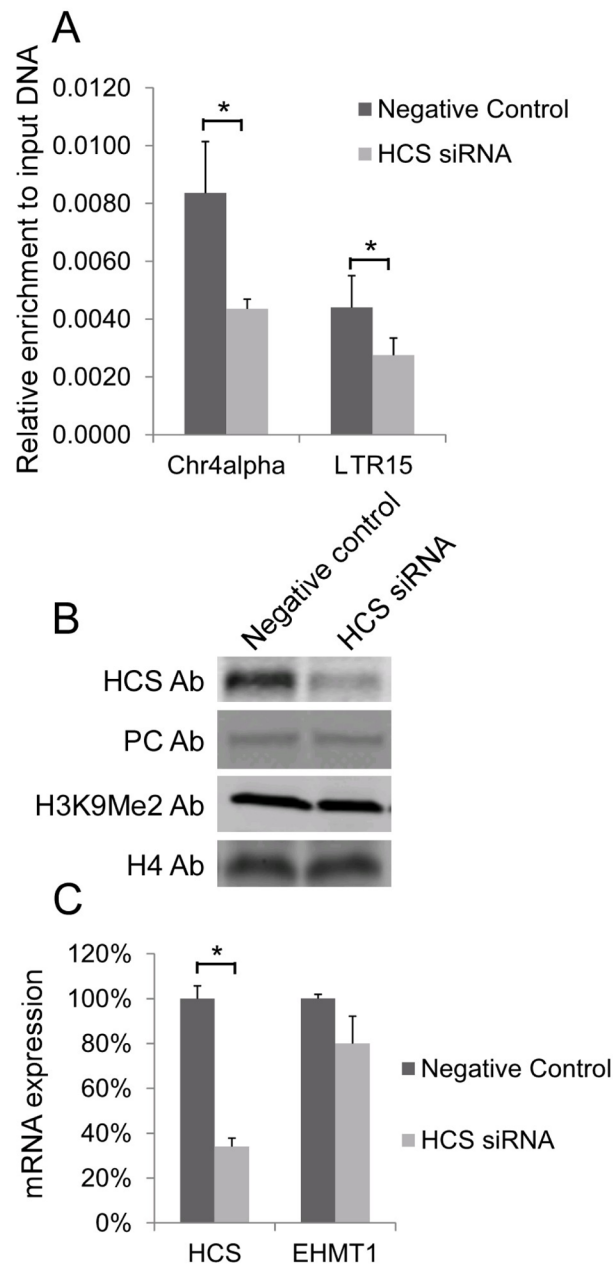
EHMT1 slows the tryptic digestion of HCS in limited proteolysis assays. Full-length recombinant human HCS was mixed with equal amount of recombinant EHMT1N-terminus, ankyrin domain, or SET domain at 37°C for 1 h. Trypsin was added and HCS degradation was monitored at timed intervals by staining gels with coomassie blue.

**Fig 5.**

EHMT1 is a target for biotinylation by HCS. (A) Recombinant N-terminus, ankyrin repeat domain, and SET domain in EHMT1 were incubated with recombinant HCS, biotin, and cofactors. EHMT1-bound biotin was probed at timed intervals. (B) Mutation of K161 and deletion of the GGAGKG motif in the EHMT1 N-terminus cause a considerable decrease in the biotinylation signal compared with the wild-type N-terminus. (C) Percent decrease of the biotinylation signal in EHMT1 mutants compared with the wild-type N-terminus. Values represent the gel densitometry signal in the streptavidin blot normalized by gel densitometry signal for the coomassie blue stain, and are reported as means \pm SD (n=3; * P <0.05).

**Fig 6.**

The K161R mutant and the GGAGKG deletion in the EHMT1 N-terminus weaken the physical interactions with HCS compared with the wild-type N-terminus. Recombinant EHMT1 proteins were incubated with recombinant HCS prior to tryptic digestion. The rate of HCS degradation was monitored at timed intervals using gel electrophoresis and staining with coomassie blue.

**Fig 7.**

HCS knockdown causes a decrease of H3K9me2 marks in repeat regions in HEK293 cells. (A) The enrichment of H3K9me2 marks in pericentromeric alpha satellite repeats and long terminal repeat 15 was quantified by chromatin immunoprecipitation assays and quantitative real-time PCR in HCS knockdown and control HEK293 cells. Values are means \pm SD (n=3; * P <0.05). (B) The abundance of HCS and (total cell) H3K9me2 was quantified by western blot analysis in HCS knockdown and control HEK293 cells. Pyruvate carboxylase (PC) and histone H4 (H4) were used as loading controls. (C) The abundance of mRNA coding for HCS and EHMT1 was quantified by quantitative real-time PCR in HCS knockdown and control HEK293 cells. Values are means \pm SD (n=3; * P <0.05).